DEVELOPMENT OF A TURBULENT SPOT INTO A STRIPE PATTERN IN PLANE POISEUILLE FLOW

Hiroshi Aida
Department of Mechanical Engineering
Tokyo University of Science
Chiba, Japan
j7510601@ed.noda.tus.ac.jp

Takahiro Tsukahara
Department of Mechanical Engineering
Tokyo University of Science
Chiba, Japan
tsuka@rs.noda.tus.ac.jp

Yasuo Kawaguchi
Department of Mechanical Engineering
Tokyo University of Science
Chiba, Japan
yasuo@rs.noda.tus.ac.jp

ABSTRACT

A structure consisting of quasi-laminar and turbulent regions in a stripe pattern, which can be found in a transitional plane channel flow, is called 'turbulent stripe'. In the previous works, the emergence of this structure was confirmed only in the case of decreasing Reynolds number from turbulent regime. In the present study, its formation from a turbulent spot has been investigated using a direct numerical simulation in a relatively large-scale computational domain of $L_x \times L_y \times L_z = 731.4\delta \times 2\delta \times 365.7\delta$ at $\mathrm{Re}_\tau = 56$ and $L_x \times L_y \times L_z = 640\delta \times 2\delta \times 320\delta$ at $\mathrm{Re}_\tau = 64$. We observed the stripe pattern of quasi-laminar and turbulent regions inside of the spot. However, the turbulent eddies decayed more rapidly for $\mathrm{Re}_\tau = 56$ than those for $\mathrm{Re}_\tau = 64$. The developed spot at $\mathrm{Re}_\tau = 64$ was found to be different form from that at $\mathrm{Re}_\tau = 56$.

INTRODUCTION

Through a direct numerical simulation (DNS), Tsukahara *et al.* (2005, 2007, 2009) found a structure consisting of quasi-laminar and turbulent regions in the stripe arrangement in a transitional plane channel flow ($\mathrm{Re}_\tau = u_\tau\delta/\nu \leq 80$, Re_τ is the friction Reynolds number, u_τ is the friction velocity, δ is the channel half width, and ν is the kinematic viscosity). This structure was named a turbulent stripe. The emergence of this structure was also verified experimentally by Hashimoto *et al.* (2009) for the bulk Reynolds number ranging from $\mathrm{Re}_\mathrm{m} = 2u_\mathrm{m}\delta/\nu = 1700$ to 2000, where u_m is the bulk mean velocity. Such localized, disordered motion is similar to a turbulent equilibrium puff in a transitional pipe flow. While a puff has been referred to as an incomplete relaminarization process Wygnanski *et al.* (1973, 1975), a slug in a pipe was associated with the transition from laminar to turbulent flow. As for the channel flow, the emergence of the turbulent stripe has been confirmed in previous studies only in the case of decreasing Reynolds number (using a fully-developed turbulent flow at a moderate Reynolds number as an initial condition). Recently, Duguet *et al.* (2010) observed the flow-field development into the turbulent stripe in a plane Couette flow, that was triggered by initial random disturbances. Their DNS studies further demonstrated that a spreading spot in the transitional regime reproduces spatio-temporal intermittency structures, such as turbulent bands. This work points out that turbulent stripe always emerge in the transitional plane Couette flow without hysteresis. In the plane Poiseuille flow, it can be anticipated that the turbulent stripe should develop from a turbulent spot in the transitional Reynolds-number regime. Nonetheless, there have been few attempts to track the growth of a single turbulent spot over a long time. Therefore, we performed DNSs of growth of a turbulent spot in the plane Poiseuille flow. In this paper, although the present work is a continuation of our previous DNS (Aida *et al.*, 2010), we report additional DNS results and discuss the formation of turbulence pattern from a spot with emphasis on its Reynolds-number dependence.

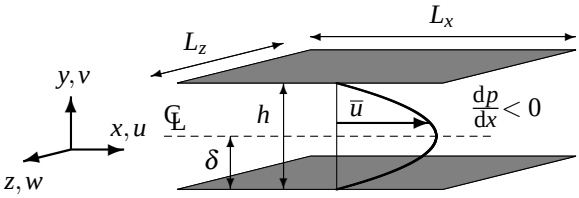

Figure 1. Configuration of channel flow.

NUMERICAL PROCEDURE

The mean flow under consideration was a plane Poiseuille flow driven by a uniform pressure gradient, as shown in Fig. 1. The periodic boundary condition was im-

Table 1. Computational conditions: L_i, domain size; N_i, number of grids; Δx_i, grid resolution; and Δt, time step.

Re_τ	$L_x \times L_y \times L_z$	$N_x \times N_y \times N_z$	Δx^+, Δz^+	Δy^+_{max}	Δy^+_{min}	Δt^+
56	$731.4\delta \times 2\delta \times 365.7\delta$	$4096 \times 64 \times 2048$	10.0	3.54	0.295	0.0224
64	$640\delta \times 2\delta \times 320\delta$			4.05	0.337	0.0128

posed in the horizontal (x, z-) directions and the non-slip condition was applied on the walls. The coordinates and flow variables were normalized by u_τ, δ, and ν. The fundamental equations were the continuity equation and the Navier-Stokes equation:

$$\frac{\partial u_i}{\partial x_i} = 0, \tag{1}$$

$$\frac{\partial u_i^+}{\partial t^*} + u_j^+ \frac{\partial u_i^+}{\partial x_j^*} = -\frac{\partial p^+}{\partial x_i^*} + \frac{1}{Re_\tau}\frac{\partial^2 u_i^+}{\partial x_j^{*2}} + \delta_{1i}, \tag{2}$$

where δ_{1i} corresponds to the mean pressure gradient and quantities with the superscript of * indicate those normalized by the outer variables, e.g., $x^* = x/\delta$, and the superscript of $^+$ indicates the normalization by the inner variables, e.g., $u^+ = u/u_\tau$. For the spatial discretization, the finite difference method was adopted. The numerical scheme with the 4th-order accuracy was employed in the streamwise and spanwise directions, while the one with the 2nd-order was applied in the wall-normal (y-) direction. Time advancement was executed by a semi-implicit scheme: the 2nd-order Crank-Nicolson method for the viscous term in the wall-normal direction and the 2nd-order Adams-Bashforth method for the other terms. Uniform grid mesh was used in the horizontal directions, and non-uniform mesh in the wall-normal direction. The friction Reynolds number was fixed to be 56 and 64, at which the turbulent stripe was found to emerge spontaneously in an initially fully turbulent flow (when the Reynolds number was decreased from the turbulent regime). Other detailed numerical conditions are summarized in Table 1. We employed relatively large-scale computational domains of $L_x \times L_y \times L_z = 731.4\delta \times 2\delta \times 365.7\delta$ at $\mathrm{Re}_\tau = u_\tau \delta/\nu = 56$ and of $L_x \times L_y \times L_z = 640\delta \times 2\delta \times 320\delta$ at $\mathrm{Re}_\tau = 64$ with $4096 \times 64 \times 2048$ grids. Such a large size of the domain allows us to consider a growing spot is not affected by neighboring spots resulting from the periodic boundary conditions, at least in the early stage of its spatial development.

A laminar flow field was used as the initial condition. The turbulent spot was triggered by a vortex pair, which had the following analytical form:

$$\left.\begin{aligned} \psi &= A\left(1-y^2\right)^2 z e^{-x^2-z^2}, \\ u &= 0, \\ v &= \psi_z, \\ w &= -\psi_y, \end{aligned}\right\} \tag{3}$$

where A is an amplitude coefficient and chosen such that the maximum initial wall-normal velocity is the same as the magnitude of center-line streamwise velocity of the laminar Poiseuille flow. This simple double-vortex disturbance was adapted by Henningson & Kim (1991). It has been known from experimental investigations of spots in various types of flows that the spot characteristics become essentially independent of the initial disturbance if its magnitude is strong enough to develop.

RESULT AND DISCUSSION

Instantaneous Velocity

Figure 2 shows instantaneous distributions of wall-normal velocity ($v^+ = v/u_\tau$) in the (x^*, z^*)-plane at the channel center, presenting a temporal evolution of a turbulent spot. Figure 2(a) shows the flow field at $\mathrm{Re}_\tau = 56$. We observed that, in the first stage of development, the vortex pair as the initial disturbance broke down and developed into a well-known arrowhead-shaped turbulent spot as it propagated downstream (see Fig. 2(a)-1). In the downstream of the spot, a disturbed but non-turbulent region can be found, and the turbulent eddies were preceded by oblique waves. These findings are in consistent with those observed by Carlson *et al.* (1982) and Henningson *et al.* (1987). The spot changed its form into a V-shape at $t^+ = tu_\tau/\nu = 800$ (Fig. 2(a)-2). At $t^+ = 1600$, quasi-laminar regions emerged in the V-shaped turbulent region. Quasi-laminar and turbulent regions formed multiple V-shapes. After that, we can see the stripe arrangement of quasi-laminar and turbulent regions like a turbulent stripe inside of the spot (Fig. 2(a)-3). Turbulent regions began to branch at the edge of the spot, and the branching regions grew parallel to each other obliquely to the streamwise direction at an angle of 20-25 degrees (Fig. 2(a)-4). Figure 2(b) also shows a temporal evolution of a spot but for $\mathrm{Re}_\tau = 64$. The spot at $t^+ = 400$ also changed arrowhead-shape like the spot at $\mathrm{Re}_\tau = 56$ (Fig. 2(b)-1). However, the turbulent eddies hardly ever decayed in the downstream region at $t^+ = 800$ (Fig. 2(b)-2). Moreover, the turbulent region developed significantly in the upstream region as well as downstream region and changed into a different form from the spot at $\mathrm{Re}_\tau = 56$. At $t^* = 3200$, the intermittent turbulent region existed inside the spot but few branching turbulent regions can be seen at the edge of the spot. It should be noted that, at $\mathrm{Re}_\tau = 56$, turbulence decayed and quasi-laminar regions emerged more significantly compared with the case at $\mathrm{Re}_\tau = 64$. It allowed the spot to change into several bands of turbulence and each turbulent bands developed parallel to each other with preceded by oblique waves.

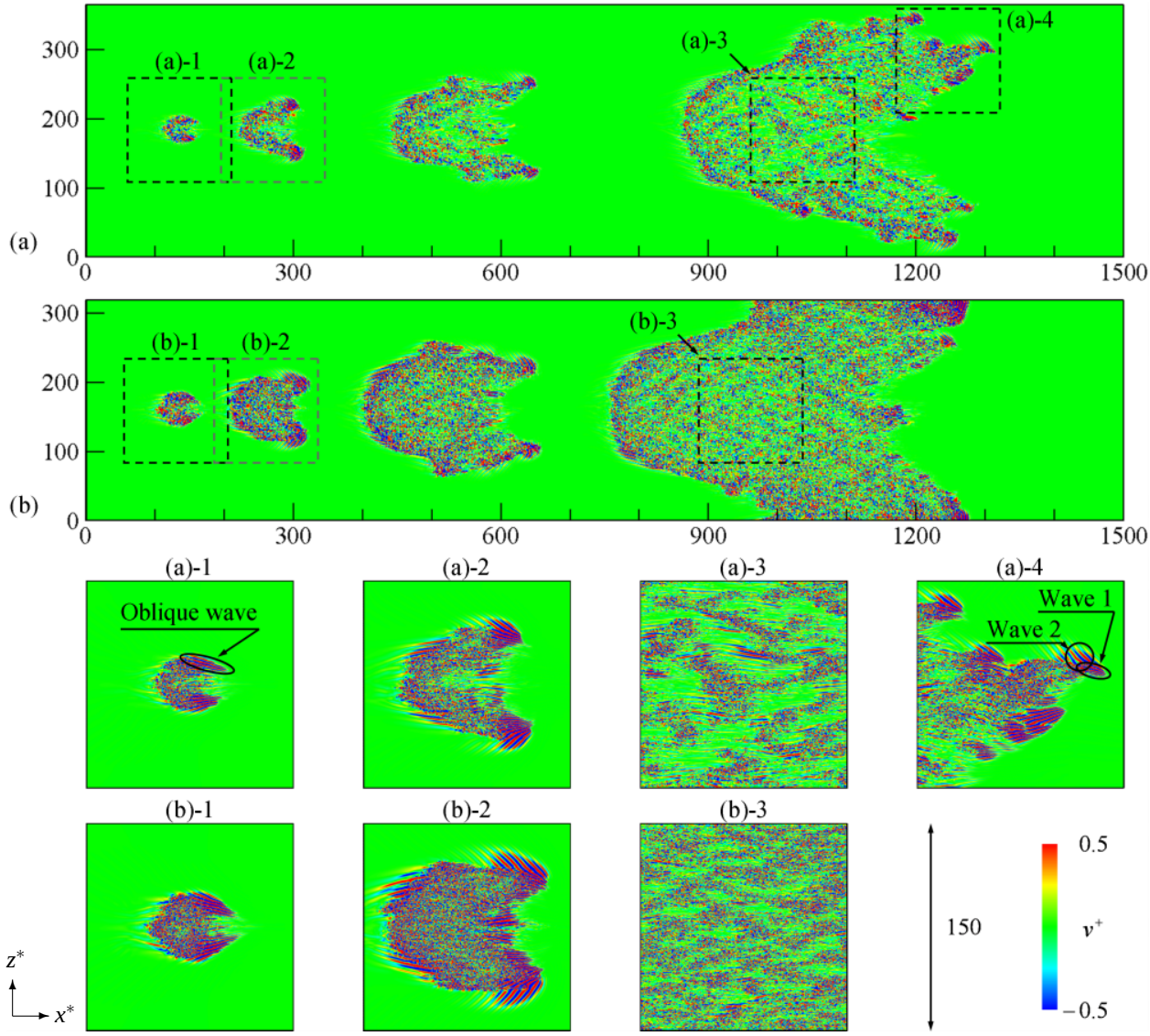

Figure 2. Contours of instantaneous wall-normal velocity in the (x^*, z^*)-plane at the channel center at $t^+ = 400$, 800, 1600 and 3200: (a) $\mathrm{Re}_\tau = 56$; (b) $\mathrm{Re}_\tau = 64$. (a)-1, (a)-2, (a)-3, (a)-4, (b)-1, (b)-2 and (b)-3 are the enlarged views of the region within the dashed box in (a) and (b).

Spreading of Disturbance

We defined three points on the spot to discuss the propagation velocity of the spot. Point x_d^* represents the streamwise position of the front (downstream) interface of the spot, point x_u^* the rear (upstream) interface, and point z^* the spanwise interfaces (refer to Fig. 3). The propagation of the spot was plotted as a function of time (t^+) in Fig. 4. As shown in Fig. 4, all points are seen to fall on straight lines, showing that their respective spot features propagate at constant speeds although turbulent region splits into quasi-laminar and turbulent regions inside of the spot. The propagation velocity of x_u^* at $\mathrm{Re}_\tau = 64$ is slower than that at $\mathrm{Re}_\tau = 56$, although the propagation velocities of x_d^* and z^* are almost independent of the Reynolds number. It means that the spot at $\mathrm{Re}_\tau = 64$ developed more significantly in the upstream region than at $\mathrm{Re}_\tau = 56$, and it results in the different form from the V-shape spot at $\mathrm{Re}_\tau = 56$.

Time Evolution of Turbulent Regions

Toh & Itano (2005) traced the spanwise movement and generation of both near-wall and large-scale structures by plotting time evolution of the spanwise locations of low-speed regions. They demonstrated that, when an interval between near-wall streak structures exceeds some critical length of the order of 100 wall units, a new wall streak emerges between the separated streaks. In our study, a similar behavior can be found in large-scale motions of the order of about 20δ, that is, a new turbulent region emerged spontaneously from quasi-laminar region between the separated turbulent bands as the spot developed. This is illustrated in Fig. 5. The contour shows the spanwise distribution of the wall-normal ve-

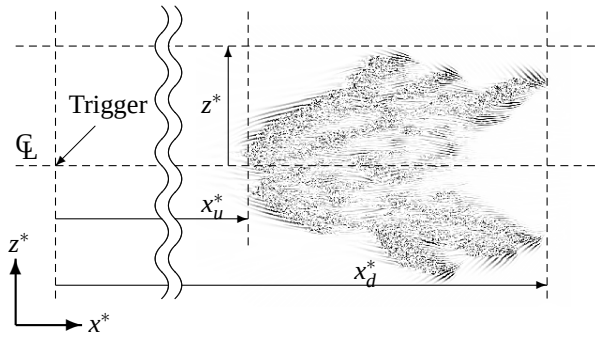

Figure 3. Turbulent-spot nomenclature.

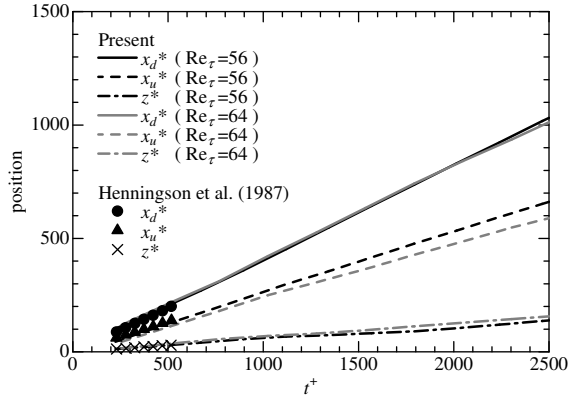

Figure 4. Position of the spot features: x_d^* and x_u^*, front and rear interfaces, respectively; z, spanwise interface.

locity at the center of the spot ($x^* = \left(x_d^* + x_u^*\right)/2$, refer to Fig. 3) and the channel center ($y^* = 1$), with time in the vertical axis. At $t^+ = 0$, a turbulent region emerged with an initial disturbance. Growing to a size of 20δ in the spanwise direction, the localized turbulent region split into two parts and a quasi-laminar region emerged between them in Fig. 5(a). The quasi-laminar region spread and then a new localized turbulent region emerged inside the quasi-laminar region. It can be said that when one (either laminar or turbulent) region develops larger in the spanwise direction than some threshold, the other region emerges to keep the spanwise spacing of each region almost constant. At $\mathrm{Re}_\tau = 64$ (Fig. 5(b)), the quasi-laminar and turbulent regions also emerged as similar to those at $\mathrm{Re}_\tau = 56$. However, the turbulent regions for the higher Reynolds number spread more actively in the spanwise direction. When compared the spot shapes between the different Reynolds numbers (see Figs. 2(a) and 2(b)), its outline for $\mathrm{Re}_\tau = 64$ seems to be circular, or crescent shape as described by Henningson & Kim (1991), rather than the V-shape. Moreover, the size of the turbulent region at the downstream edge of the spot was larger compared to that at $\mathrm{Re}_\tau = 56$.

Vortex Structure

Figure 6 shows the second invariant of deformation tensor:

$$II = \frac{\partial u_i^+}{\partial x_j^*}\frac{\partial u_j^+}{\partial x_i^*} \qquad (4)$$

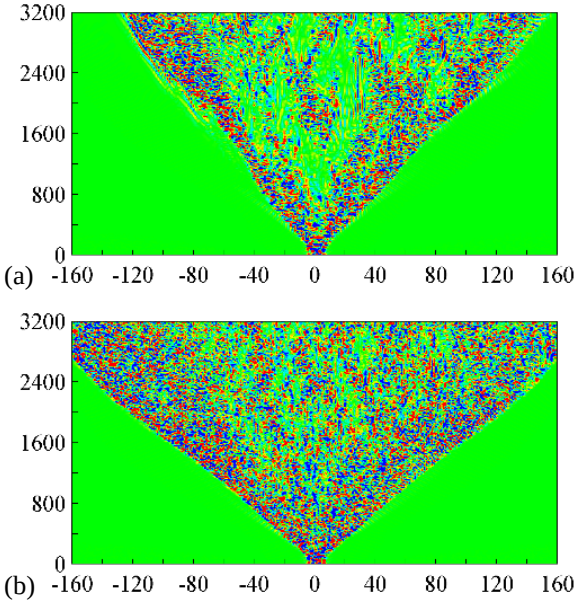

Figure 5. Space-time (z^*-t^+) plot of wall-normal velocity (v^+) showing the formation of a turbulent-laminar pattern: (a) $\mathrm{Re}_\tau = 56$; (b) $\mathrm{Re}_\tau = 64$.

at (a) $t^+ = 400$ and (b) 800 for $\mathrm{Re}_\tau = 56$ and at (c) $t^+ = 400$ and (d) 800 for $\mathrm{Re}_\tau = 64$. It can be easily found that no vortex can be seen in the downstream of the spot and vortex cluster takes a V-shape. Figure 6(e)-(g) are the enlarged views of the regions within the box in (a), (b) and (d). In Fig. 6(e), elongated vortices at the wing-tip regions were found, and they were staggered in (y-z)-plane. It is considered that the staggered alignment of the vortices induced the oblique waves and make their wavelength to be about twice of the channel height as reported by Alavyoon *et al.* (1986). There could also be seen a few elongated vortices in the upstream region of the spot for $\mathrm{Re}_\tau = 64$ (Fig. 6(g)) but they are absent for $\mathrm{Re}_\tau = 56$ (Fig. 6(f)). For both cases, the oblique waves obviously appeared at the downstream of the spot, as seen in Fig. 6(e). However, the structure of the upstream oblique waves seem different from the downstream one. Sparse regions can be found inside the V-shape spot, as shown in Fig. 6(b) and (d). These regions developed into quasi-laminar regions inside the spot.

Mechanism of Transition

Figures 7(b)-(d) show temporal changing of the streamwise velocity in the (x^*, y^*)-plane at $t^+ = 800$, 850 and 900. High-speed (laminar) flow impinges on downstream low-speed (turbulent) flow and curved into one side of the channel, as shown in (b). Low-speed flow near the other side of the walls was induced into the channel center (see red box in (c)). Figures 7(e)-(g) are the enlarged views of the region within the red box in (b)-(d), respectively, with vectors showing streamwise ($u^+ - u^+_{\mathrm{m,laminar}}$) and wall-normal ($v^+$) velocities. Here, $u^+_{\mathrm{m,laminar}}$ denotes the bulk mean velocity of laminar region. The velocity gradient in the channel-central region is increased by low-speed flow blowing into the channel cen-

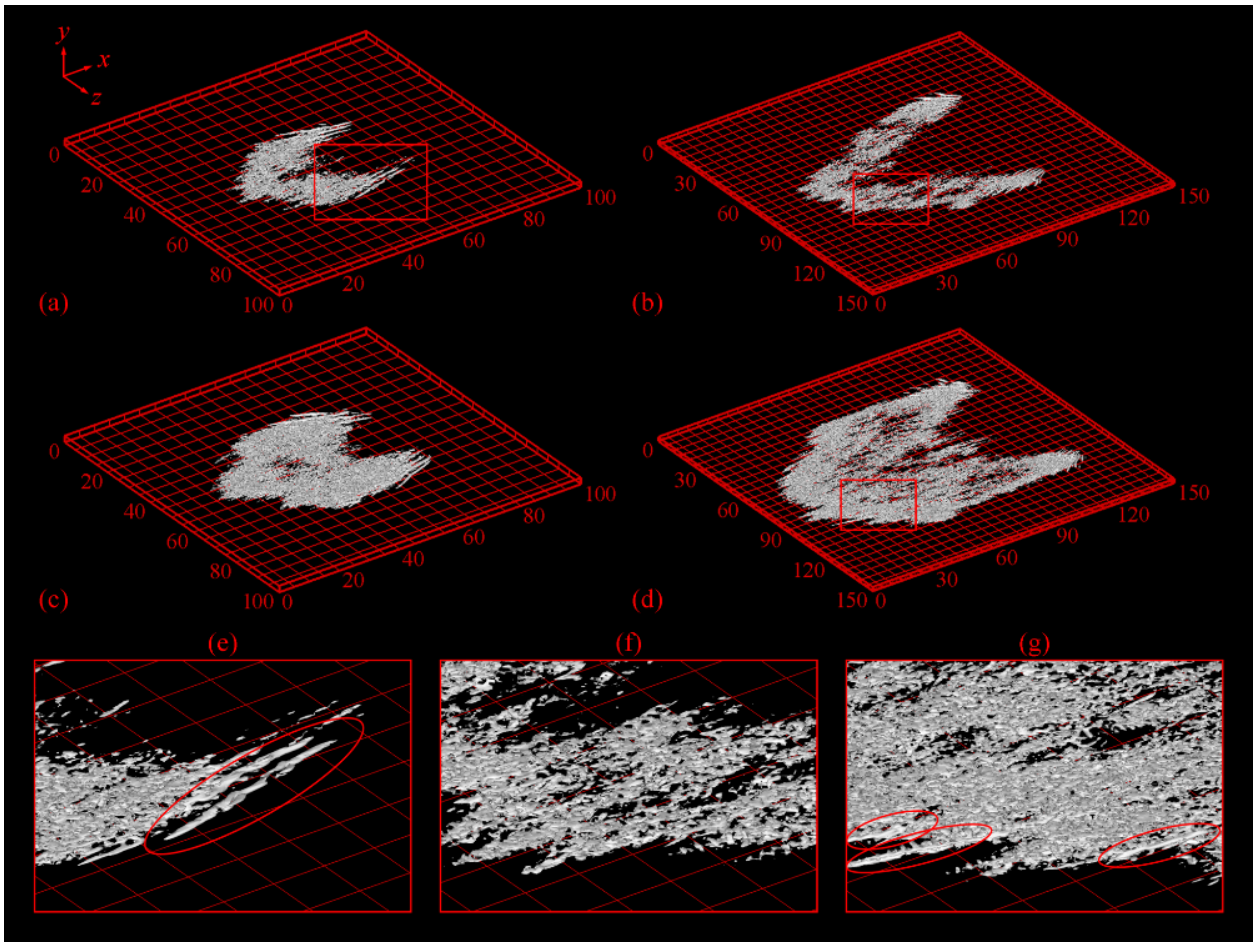

Figure 6. Iso-surfaces of second invariant of deformation tensor ($II^+ = u^+_{i,j}u^+_{j,i}$), which is equivalent to the vortical position. The direction of the mean flow is from bottom-left to top-right. (a) $t^+ = 400$, (b) $t^+ = 800$ at $\mathrm{Re}_\tau = 56$; (c) $t^+ = 400$, (d) $t^+ = 800$ at $\mathrm{Re}_\tau = 64$. (e) and (f) are the enlarged views of the region within the box in (a) and (c).

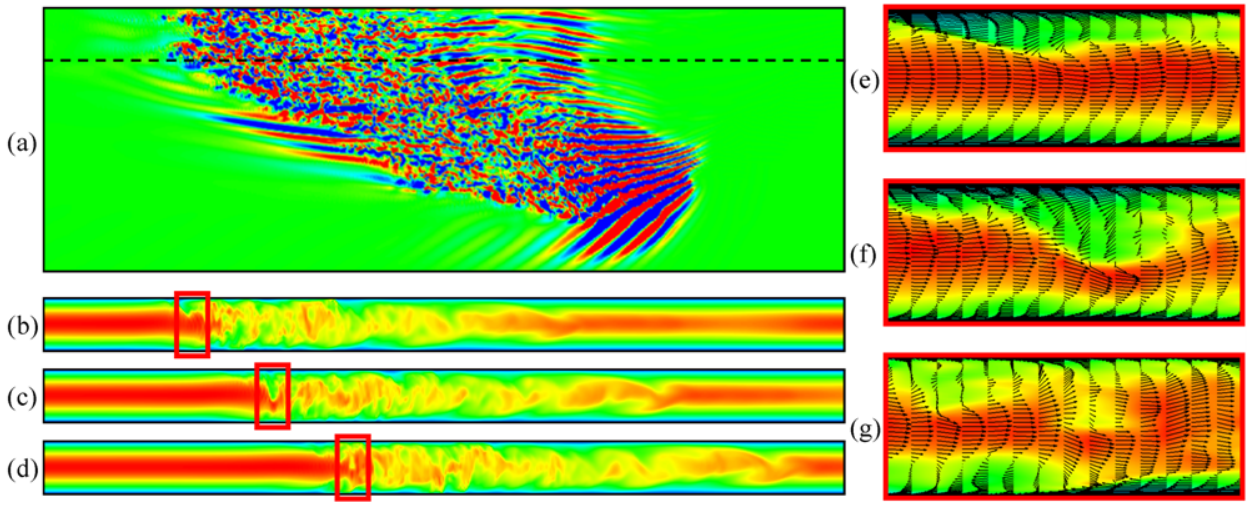

Figure 7. (a) Same as Fig. 2(a)-2, but for the visualized volume is $150\delta \times 50\delta$. (b)-(d) Contours of instantaneous streamwise velocity in the (x^*, y^*)-plane at the positions of the dashed line in (a), at $t^+ = 800$, 850 and 900. Contour colour ranges from blue to red [0, 28]. The visualized volume is $150\delta \times 2\delta$, but aspect ratio of x to y-direction is 0.2. (e)-(g) are the enlarged views of the region within the red box in (b)-(d) with vectors showing streamwise ($u^+ - u^+_{\mathrm{m,laminar}}$) and wall-normal ($v^+$) velocities, but aspect ration of x to y-direction is 1.

ter. Then due to the Kelvin-Helmholtz (K-H) instability, it gives rise to many vortices, as shown in Fig. 7(d), and induces the transition from laminar to turbulence near the interface, but inside the spot. This aspect is similar to the driving mechanism of a turbulent puff, proposed by Shimizu & Kida (2009), who studied a circular pipe flow by tracing temporal changing of low-speed streaks and vortex layers. At another position of the upstream spot interface which is accompanied by the oblique waves, an oncoming high-speed flow region is curved and meandered in the *y* direction more significantly (figure not shown), compared with that observed in Fig. 7. It is conjectured that the high-speed motion approaching the spot interface should be decelerated with giving rise to the oblique waves. Here, the existence of oblique waves can be interpreted as the appearance of longitudinal vortex packets. As shown in Fig. 6(g), a few of elongated streamwise vortices are, indeed, clearly confirmed in the upstream interface of the spot for $\mathrm{Re}_\tau = 64$, while they are absent or very weak for $\mathrm{Re}_\tau = 56$. It implies that the momentum transfer from the mean to these vortices is large in the higher Reynolds-number flow. Therefore, the transition at the upstream region of the spot at $\mathrm{Re}_\tau = 56$ is slower than that at $\mathrm{Re}_\tau = 64$.

CONCLUSION

In the present study, we performed large-scale DNSs on a turbulent spot developing into turbulent stripes in a channel flow at the transitional Reynolds-number regime (particularly, at $\mathrm{Re}_\tau = 56$ and 64). We found that the spot developed in the form of stripe arrangements of quasi-laminar and turbulent regions inside of the spot, while keeping each region almost constant in scale. We observed different oblique waves at the edge of the developed spot from those observed in the arrowhead-shaped one. The turbulent regions also exist intermittently inside a spot at $\mathrm{Re}_\tau = 64$. However, the Reynolds-number dependences of the development- and decay-rates of turbulent region, especially the highly disturbed region at the upstream interface of the growing spot, allows the spot itself to be different forms.

ACKNOWLEDGMENT

The present computations were performed with the use of the supercomputing resources at Cyber-Science Center of Tohoku University. This work has been supported by KAKENHI (#22760136).

REFERENCES

Aida, H., Tsukahara, T. & Kawaguchi, Y. 2010 DNS of turbulent spot developing into turbulent stripe in plane Poiseuille flow. In *Proceedings of 3rd Joint US-Euro. FEDSM, FEDSM/ICNMM2010-30956*.

Alavyoon, F., Henningson, D. S. & Alfredsson, P. H. 1986 Turbulent spots in plane Poiseuille flow-flow visualization. *Phys. Fluids* **29(4)**, 1328–1331.

Carlson, D. R., Widnall, S. E. & Peeters, M. F. 1982 A flow-visualization study of transition in plane poiseuille flow. *J. Fluid Mech.* **121**, 487–505.

Duguet, Y., Schlatter, P. & Henningson, D. S. 2010 Formation of turbulent patterns near the onset of transition in plane Couette flow. *J. Fluid Mech.* **650**, 119–129.

Hashimoto, S., Hasobe, A., Tsukahara, T., Kawaguchi, Y. & Kawamura, H. 2009 Experimental study on turbulentstripe structure in transitional channel flow. In *Proceedings of the Sixth International Symposium on Turbulence, Heat and Mass Transfer*, pp. 193–196.

Henningson, D., Spalart, P. & Kim, J. 1987 Numerical simulations of turbulent spots in plane Poiseuille and boundary-layer flow. *Phys. Fluids* **30**, 2914–2917.

Henningson, D. S. & Kim, J. 1991 On turbulent spots in plane Poiseuille flow. *J. Fluid Mech.* **228**, 183–205.

Shimizu, M. & Kida, S. 2009 A driving mechanism of a turbulent puff in pipe flow. *Fluid Dyn. Res.* **41**, 045501.

Toh, S. & Itano, T. 2005 Interaction between a large-scale structure and near-wall structure in channel flow. *J. Fluid Mech.* **524**, 249–262.

Tsukahara, T., Kawaguchi, Y., Kawamura, H., Tillmark, N. & Alfredsson, P. H. 2009 Turbulence stripe in transitional channel flow with/without system rotation. In *Proceedings of the Seventh IUTAM Symposium on Laminar-Turbulent Transition, Vol. 18 of IUTAM Bookseries* (ed. P. Schlatter & D. Henningson), pp. 421–426. Springer.

Tsukahara, T. & Kawamura, H. 2007 Turbulent heat transfer in a channel flow at transitional Reynolds numbers. In *the First Asian Symposium on Computational Heat Transfer and Fluid Flow*, p. 62.

Tsukahara, T., Seki, Y., Kawamura, H. & Tochio, D. 2005 DNS of turbulent channel flow at very low Reynolds numbers. In *Proceedings of Fourth International Symposium on Turbulence and Shear Flow Phenomena* (ed. L. J. S. Bradbury *et al.*), pp. 935–940.

Wygnanski, I. J. & Champagne, F. H. 1973 On transition in a pipe. Part 1. the origin of puffs and slugs and the flow in a turbulent slug. *J. Fluid Mech.* **59**, 281–335.

Wygnanski, I. J., Sokolov, M. & Friedman, D. 1975 On transition in a pipe. Part2 the equilibrium puff. *J. Fluid Mech.* **69**, 283–304.